

NOISE AND MODULATION EXPERIMENTS ON CATHODOLUMINESCENCE FROM ZnS–Ag

H. M. FIJNAUT and J. F. VAN DER VEEKEN
Fysisch Laboratorium, Utrecht, Nederland

Received 21 July 1971

Synopsis

The concept of luminescence from donor–acceptor transitions, introduced by Williams¹), was applied to calculations of a.c. modulation response, spectral noise density, and emission spectrum of the radiation. These calculations were based on a donor–acceptor transition probability that decreases exponentially with their separation²), whereas donors and acceptors were assumed to be randomly distributed over the phosphor. The distribution of de-excitation probabilities was approximated by taking into account the statistical distribution in space of nearest neighbours only. The frequency dependence of squared a.c. modulation response (SMR) and spectral noise density (SND) were found to be identical at low excitation densities, whereas the frequency dependence of the SMR for a selected narrow wavelength band out of the emission spectrum was calculated to vary with wavelength.

Our theoretical results were compared with experiments on cathodoluminescence from ZnS–Ag, while some experimental results of Era *et al.* concerning the shift in the peak position of the emission with excitation density, were compared with our theoretical predictions. The agreement found gives an additional proof of the existence of the donor–acceptor mechanism for the blue luminescence of ZnS–Ag.

1. *Introduction.* In this paper we are dealing with some experiments on cathodoluminescence of ZnS–Ag. In numerous foregoing papers the broad-band luminescence of ZnS type phosphors due to activators (determining the emission spectrum, here Ib elements) and coactivators (characteristic for the efficiency of the luminescence, here III b and VII b elements) has been reported and information about the different mechanisms involved has been obtained. Much work has been done in order to clarify the relation between preparation conditions of the phosphor and the resulting luminescence. A classification of the broad-band luminescence according to the ratio of activator–coactivator concentrations has been presented by van Gool⁴). Five luminescence mechanisms have been distinguished, each with characteristic peaks in the emission spectrum. Comparing our emission spectrum (see fig. 6) with spectra of van Gool⁴) and Era *et al.*³) our phosphors appear to belong to the so-called green Cu type, *i.e.* the coactivator

concentration equals or is somewhat larger than the activator concentration. A review of the luminescence of the ZnS-type phosphors has been given by Shionoya^{5,6}).

For the green Cu-type luminescence, Prener and Williams⁷) and Apple and Williams⁸) have suggested the mechanism of donor-acceptor emission. It has been assumed that luminescent recombinations occur of electrons bound on donors with holes bound on acceptors. In this case the recombination energy depends on the energy of donor and acceptor states involved as well as on the Coulomb interaction between electron on donor and hole on acceptor. As a consequence the transition *energy* depends on the spatial separation of donor and acceptor. In addition, the transition *probability* is also a function of the separation of donor and acceptor and therefore one may expect a specific relation between emitted wavelength and transition probability. Some features of donor-acceptor recombination in semiconductors have been reviewed by Williams⁹).

Thomas *et al.*²) have found that the donor-acceptor emission actually occurs in GaP. Its green emission was composed of a large number of sharp lines, which could be associated with the allowed, discrete separations of donors and acceptors at specific lattice sites. Recently, Era *et al.*³) have investigated the blue ZnS-Ag luminescence (of phosphors belonging to the green Cu type). Especially, measurements have been done on the emission-peak shift during decay after pulsed excitation and on the peak shifts as a function of photo-excitation intensity. Their experimental data, obtained with powder phosphors, suggest that the blue Ag luminescence in ZnS-Ag may indeed be described by donor-acceptor recombination. It must be noted here that in the case of donor-acceptor recombination the designations of activator and coactivator become meaningless in the original sense. Considering ZnS-Ag luminescence, Ag acts as acceptor, whereas Cl, In or Al act as donors.

The object of our study was to investigate quantitatively, by performing kinetic measurements, *i.e.* noise and a.c. response measurements, whether the cathodoluminescence of ZnS-Ag can be ascribed to donor-acceptor recombination. Starting from a purely random distribution of donors and acceptors over the phosphor, we calculated the a.c. luminescence response on a.c. modulated excitation as well as the spectral noise density of the luminescence. In addition, the optical emission spectrum was calculated, as a function of excitation density and the calculated peak shift was compared with the experimental results of Era *et al.*³). In the calculations, stimulated emission, self-absorption and radiationless donor-acceptor recombinations were neglected.

Although we feel it as a serious omission we shall also refrain from taking phonon interaction into account, since otherwise calculations would become too cumbersome. This implies that the calculated widths of the emission

spectra are too small, as the phonon interaction is expected to widen the spectra. The calculated peak shifts, however, will not be seriously affected.

2. *Theory.* The process of donor-acceptor recombination in cathodoluminescence must be understood as follows. One, highly energetic, electron arrives at the phosphor, and creates one way or another thermalised secondaries. Next, these secondaries are bound to a donor and subsequently recombine with an acceptor hole. Finally, the electron recombines with a hole in the valence band.

According to Williams⁹⁾ the energy $E(s)$, associated with a recombination of a donor electron with an acceptor hole at distance s , is given by

$$E(s) = E_{\text{gap}} - (E_{\text{a}} + E_{\text{d}}) + e^2/\epsilon s, \quad (1)$$

where E_{gap} is the band-gap energy, E_{a} and E_{d} are the acceptor and donor binding energies, respectively, $-e$ is the electron charge and ϵ the dielectric constant. In eq. (1) the Coulomb interactions between donor electron and acceptor core, as well as those between acceptor hole and donor core are neglected. This means that eq. (1) holds only for pairs of separation larger than about 5 Å.

If either acceptor or donor has a small binding energy, the transition probability $W(s)$ for donor electron to an acceptor hole at distance s is given by²⁾

$$W(s) = W_{\text{m}} \exp(-s/s_{\text{d}}), \quad (2)$$

where W_{m} is constant and s_{d} is half the Bohr radius of the level with least binding energy. In the case of blue Ag luminescence the Ag level is fairly deep and the donor level is shallow and hydrogenic³⁾. It seems therefore reasonable in our case to use the transition probability of eq. (2).

In order to perform calculations on a system of donors and acceptors a spatial distribution of their positions must be assumed. As an approximation we assume a random distribution of donors and acceptors in space. On this basis we shall calculate the distribution of transition probabilities. First we calculate the nearest-neighbour distribution $P(s)$ from two combined probabilities concerning donor and acceptor positions: the probability that one acceptor is between two concentric spheres of radius s and $s + ds$ around the donor and that there is no acceptor within the sphere of radius s is:

$$P(s) ds = \frac{4\pi s^2}{V} N_{\text{a}} ds \left(1 - \int_0^s \frac{4\pi s'^2}{V} ds' \right)^{N_{\text{a}}-1},$$

where V is the volume and N_{a} the number of acceptors within V . In the limit $N_{\text{a}} \rightarrow \infty$, $V \rightarrow \infty$ but keeping the acceptor concentration $n_{\text{a}} = N_{\text{a}}/V$

constant, one finds:

$$P(s) ds = 4\pi s^2 n_a \exp(-\frac{4}{3}\pi n_a s^3) ds, \quad (3)$$

(see also Williams⁹).

The total donor-acceptor transition probability is the sum of the probabilities of transitions of the donor to the acceptor in the shell ($s, s + ds$) and to all acceptors outside the sphere with radius s . We now assume as a further approximation that the acceptors outside the sphere are homogeneously and smoothly distributed so that the total transition probability $T(s)$ for the donor is: $T(s) = W(s) + \int_s^\infty 4\pi n_a x^2 W(x) dx$, and from eq. (2):

$$T(s) = W_m \{1 + 4\pi n_a s_d^3 [(s/s_d)^2 + 2(s/s_d) + 2]\} \exp(-s/s_d). \quad (4)$$

In order to verify the validity of the simplification made by assuming the homogeneous distribution, the distribution of transition probabilities, found by combination of eqs. (3) and (4), was compared with the more exact distribution found by a computer programmed to simulate our problem. This was done by generating random points in an imaginary crystal, centered around an imaginary donor, and calculating the total

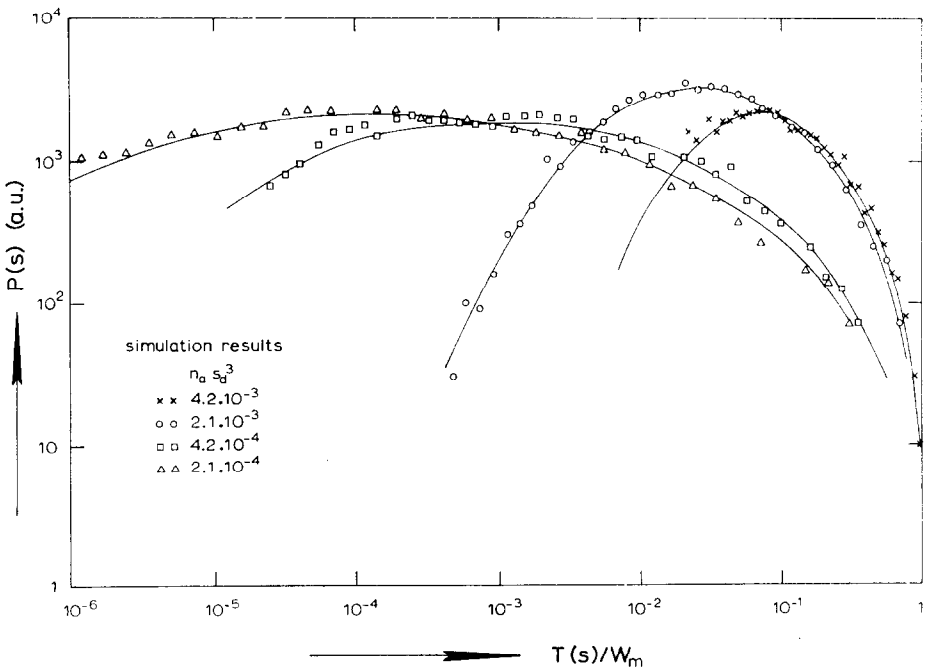


Fig. 1. Comparison of transition probability distributions, calculated from eqs. (3) and (4) (drawn curves) and found from computer simulations, for different values of $N_a s_d^3$. Results of the computer simulations were fitted along the vertical axis.

transition probability to the random points as a sum of the probabilities given by eq. (2). The results are shown in fig. 1, and justify the approximation in the transition probability $T(s)$ according to eq. (4) for the range of values of $n_a s_d^3$ considered.

Let the actual number of electron-occupied donors, with nearest acceptor between s and $s + ds$, be $N(s, t) ds$, then its time dependence is described by:

$$\frac{\partial}{\partial t} N(s, t) ds = g(s, t) ds - r(s, t) ds, \quad (5a)$$

where $g(s, t) ds$ and $r(s, t) ds$ are the excitation and de-excitation rates, respectively. We assume that the de-excitation process is monomolecular, hence:

$$r(s, t) = T(s) N(s, t), \quad (5b)$$

if the time during which the electron is on the acceptor is short compared to the lifetimes of the electron-occupied donors, and de-excitations only occur by donor-acceptor recombination. In addition, we may write:

$$g(s, t) = g(t)[N_d(s) - N(s, t)], \quad (5c)$$

where $N_d(s) ds$ is the number of donors with nearest acceptor between s and $s + ds$, and $g(t)$ is the excitation rate for all empty donors, depending on the electron flux incident on the phosphor. For a correct manner of writing of $g(s, t)$ see appendix of ref. 10.

In noise and modulation measurements we are interested in the a.c. behaviour of our luminescence mechanism. Considering small deviations from the steady state, denoted by Δ , we may write:

$$N(s, t) = \overline{N(s, t)} + \Delta N(s, t),$$

$$g(t) = \langle g(t) \rangle + \Delta g(t),$$

$$r(s, t) = \overline{r(s, t)} + \Delta r(s, t),$$

where horizontal bars and brackets denote time and ensemble averages respectively. We now find from eq. (5) to first order of ΔN :

$$\frac{\partial}{\partial t} \Delta N(s, t) + \alpha(s) \Delta N(s, t) = G(s, t) - R(s, t), \quad (6a)$$

where

$$\Delta r(s, t) = T(s) \Delta N(s, t) + R(s, t),$$

$$\alpha(s) = T(s) + \langle g(t) \rangle, \quad (6b)$$

$$G(s, t) = \Delta g(t)[N_d(s) - \overline{N(s, t)}].$$

The a.c. excitation and de-excitation processes are described by the source

terms $G(s, t)$ and $R(s, t)$ respectively. When fluctuations are considered, $G(s, t)$ and $R(s, t)$ represent stochastic source functions, the time dependence of which is not predictable, but about the statistical properties of which reasonable assumptions can be made¹¹), enabling us to calculate the resulting spectral noise density of the light fluctuations. When, however, the response to a.c. modulated excitation is considered, $R(s, t)$ may be put equal to zero, whereas $G(s, t)$ describes the a.c. modulation, the time dependence of which is sinusoidal.

Denoting the Fourier transform of $x(t)$ by $a_x(\omega)$, the Fourier transformed eqs. (6a) and (6b) become:

$$\begin{aligned} a_{\Delta N(s, t)}(\omega) &= [a_{G(s, t)}(\omega) - a_{R(s, t)}(\omega)]/[j\omega + \alpha(s)], \\ a_{\Delta r(s, t)}(\omega) &= T(s) a_{\Delta N(s, t)}(\omega) + a_{R(s, t)}(\omega), \end{aligned} \quad (6c)$$

where $\omega = 2\pi f$, f is frequency, and $j = \sqrt{-1}$.

2.1. Squared a.c. modulation response. Sinusoidal modulation of the exciting electron beam is represented by a sinus term in $g(t)$ and thus in $G(s, t)$. The Fourier transform of $G(s, t)$ is therefore sharply peaked around the modulation frequency. Denoting the Fourier coefficient of $G(s, t)$ at the modulation circular frequency ω by $a_{G(s, t)}(\omega) = \mathcal{P}[N_d(s) - \overline{N(s, t)}]$, according to eq. (6b), we find from eq. (6c), neglecting fluctuations *i.e.* $a_R = 0$;

$$a_{\Delta r(s, t)}(\omega) = T(s) \mathcal{P}[N_d(s) - \overline{N(s, t)}]/[j\omega + \alpha(s)]. \quad (7a)$$

From the steady-state solution of eq. (5a), we find with the help of eqs. (5b) and (5c) and using $\langle g(t) \rangle = \alpha(s) - T(s)$:

$$N_d(s) - \overline{N(s, t)} = T(s) N_d(s)/\alpha(s). \quad (7b)$$

We now define the squared modulation response SMR of the integral luminescence spectrum at frequency ω by

$$\text{SMR}(\omega) = \int_0^\infty \int_0^\infty a_{\Delta r(s, t)}(\omega) a_{\Delta r(s', t)}^*(\omega) ds ds',$$

where the asterisk denotes the complex conjugate quantity. Inserting eqs. (7a) and (7b) one finds, since the integrand with respect to s and s' factorizes:

$$\frac{\text{SMR}(\omega)}{\mathcal{P}^2 N_d^2} = \left[\int_0^\infty \frac{T^2(s) P(s)}{\alpha^2(s) + \omega^2} ds \right]^2 + \left[\omega \int_0^\infty \frac{T^2(s) P(s)}{\alpha(s) \{ \alpha^2(s) + \omega^2 \}} ds \right]^2, \quad (8)$$

where N_d is the total number of donors and thus $N_d(s) = N_d P(s)$. With the help of eq. (8) the SMR was calculated numerically for some values of $n_a s_d^3$ and $\langle g(t) \rangle / W_m$ as function of ω / W_m . The results for values of $\langle g(t) \rangle$ small with respect to $T(s)$ [eq. (6b)] are shown in fig. 2.

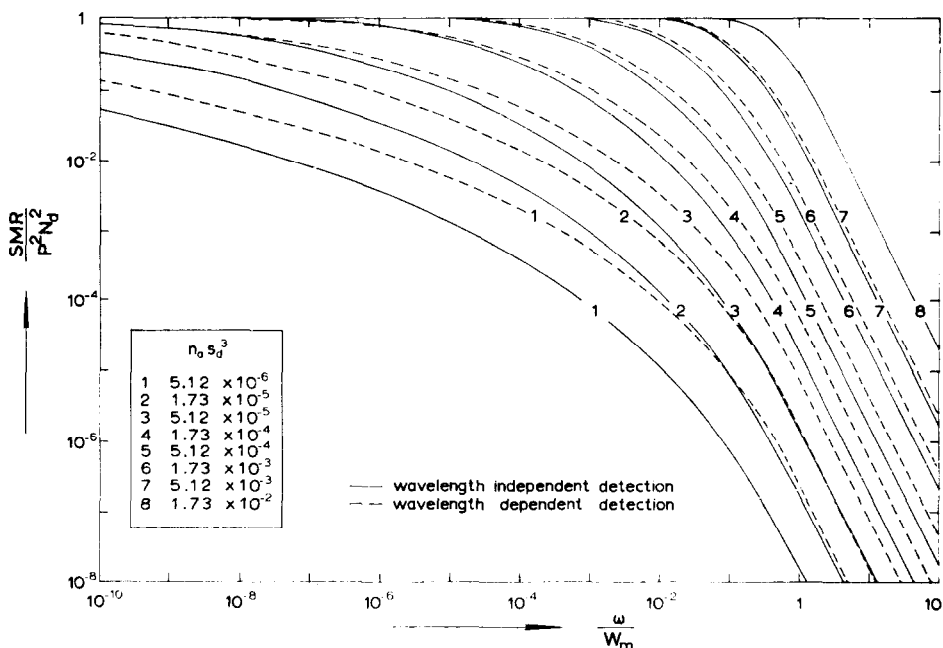


Fig. 2. SMR, as function of ω/W_m , for different values of $n_a s_d^3$, for $\langle g(t) \rangle \ll T(s)$. Drawn curves represent the case of wavelength-independent detection, whereas dashed curves show the SMR for a special case of wavelength-dependent detection (see section 2.1).

Since in the donor-acceptor recombination model the transition energy (related to wavelength) as well as the transition probability are related to the donor-acceptor separation it seemed of interest to calculate the SMR also for a certain narrow spectral band ($\lambda, \lambda + \Delta\lambda$), which corresponds to a narrow interval of separation values ($s, s + \Delta s$). Different wavelength bands should bring about different SMR curves, which can be verified experimentally. In addition we shall consider the influence of wavelength-dependent detection efficiency on the measured SMR for integral spectral emission. Let us, therefore, consider transitions between donor and acceptors with separations between s_1 and s_2 (fig. 3), corresponding to a certain wavelength interval. For donors with nearest acceptor at s , being less than s_1 , the fraction of transitions to a hole-occupied acceptor at a distance between s_1 and s_2 is:

$$\left[\int_{s_1}^{s_2} 4\pi n_a s'^2 W(s') ds' \right] / T(s).$$

For donors with nearest acceptor between s and $s + ds$ the fraction of the Fourier transform of $G(s, t)$ that contributes to transitions to acceptors between s_1 and s_2 , is, according to eq. (7b), obtained from the relations

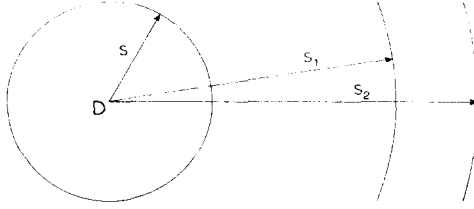


Fig. 3. Model of the phosphor, with transitions from the donor D to an acceptor between s_1 and s_2 , whereas the nearest acceptor is at distance s .

$$N_d(s) = N_d P(s) \text{ and } a_{G(s,t)}(\omega) = \dot{p}[N_d(s) - \overline{N(s,t)}]:$$

$$a_{s_1, s_2}(s, \omega) ds = \int_{s_1}^{s_2} 4\pi n_a s'^2 W(s') f(s') ds' \frac{\dot{p} N_d P(s) ds}{\alpha(s)}, \quad (9)$$

where $f(s')$ is the detected fraction of transitions from donors to acceptors with separation s' determined by the wavelength-dependent detection efficiency. For $s_1 \leq s \leq s_2$ we find:

$$a_{s_1, s_2}(s, \omega) ds = \left[W(s) f(s) + \int_s^{s_2} 4\pi n_a s'^2 f(s') W(s') ds' \right] \frac{\dot{p} N_d P(s) ds}{\alpha(s)}, \quad (10)$$

where the first term of the right-hand side follows from our assumption that one acceptor is at a distance between s and $s + ds$. The Fourier coefficient of Δr for transitions between s_1 and s_2 , $a_{\Delta r(s,t)}(s_1, s_2, \omega)$, is according, to eq. (6b), neglecting again $a_{R(s,t)}(\omega)$:

$$a_{\Delta r(s,t)}(s_1, s_2, \omega) = [a_{s_1, s_2}(s, \omega)_{\text{from eq. (9)}}] T(s) / [j\omega + \alpha(s)], \quad s < s_1 \quad (11)$$

$$[a_{s_1, s_2}(s, \omega)_{\text{from eq. (10)}}] T(s) / [j\omega + \alpha(s)],$$

$$s_1 \leq s \leq s_2.$$

For two particular cases, the SMR will now be calculated. First, the SMR for $s_1 \rightarrow 0$, $s_2 \rightarrow \infty$ and $f(s) \neq 1$, denoted by $\text{SMR}(0, \infty, \omega)$ is found to be:

$$\begin{aligned} \text{SMR}(0, \infty, \omega) = & \left[\dot{p} N_d \int_0^{\infty} \frac{4\pi n_a F(s) + W(s) f(s)}{\alpha^2(s, t) + \omega^2} T(s) P(s) ds \right]^2 \\ & + \left[\dot{p} N_d \omega \int_0^{\infty} \frac{4\pi n_a F(s) + W(s) f(s)}{\alpha^2(s, t) + \omega^2} \frac{T(s)}{\alpha(s, t)} P(s) ds \right]^2, \end{aligned} \quad (12)$$

where $F(s) = \int_0^{\infty} s'^2 f(s') W(s') ds'$. It can easily be verified that for $f(s) \equiv 1$, eqs. (12) and (8) are identical.

To calculate $\text{SMR}(0, \infty, \omega)$ assumptions about $f(s)$ have to be made. In

our experiments we used an E.M.I. 9558 photomultiplier, with S 20 cathode, as photodetector. In view of the well-known quantum efficiency of this photocathode as function of wavelength λ and the shape of the emission spectrum of ZnS-Ag (fig. 6), we approximated in our calculations the wavelength-dependent detection efficiency by a linear function of λ . The corresponding function $f(s)$ was found by means of the $E - s$ relation of eq. (1) and the relation $E = hc/\lambda$. Some numerically computed results from eq. (12) are shown in fig. 2.

Next we consider finite positive values for s_1 and s_2 , corresponding to a wavelength interval. Assuming that $f(s)$ is constant in this interval, say $f(s) \equiv f(s_1)$, we find for the SMR for the interval (s_1, s_2) , denoted by $\text{SMR}(s_1, s_2, \omega)$:

$$\begin{aligned} \text{SMR}(s_1, s_2, \omega) = & [pN_d f(s_1)]^2 \left\{ \left[[K(s_2) - K(s_1)] \int_0^{s_1} \frac{T(s) P(s)}{\alpha^2(s) + \omega^2} ds \right. \right. \\ & + \left. \int_{s_1}^{s_2} [K(s_2) - K(s) + W(s)] \frac{T(s) P(s)}{\alpha^2(s) + \omega^2} ds \right\}^2 \\ & + \left\{ [K(s_2) - K(s_1)] \omega \int_0^{s_1} \frac{T(s) P(s) ds}{\alpha(s)[\alpha^2(s) + \omega^2]} \right. \\ & \left. + \omega \int_{s_1}^{s_2} \frac{[K(s_2) - K(s) + W(s)] T(s) P(s)}{\alpha(s)[\alpha^2(s) + \omega^2]} ds \right\}^2 \end{aligned} \quad (13)$$

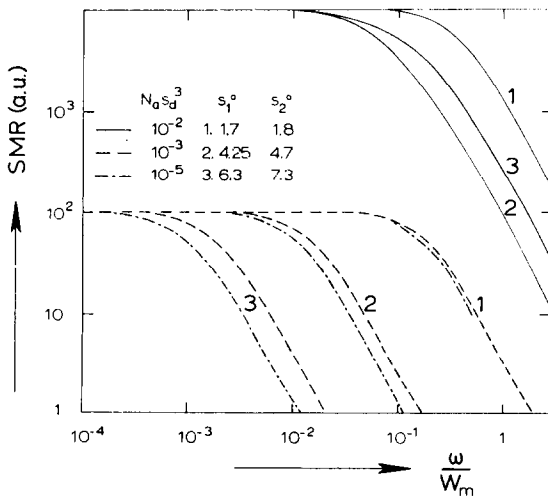


Fig. 4. SMR of wavelength bands filtered out of the emission spectrum. Calculations are based on eq. (13) while $s^0 \equiv s/s_d$.

with

$$K(s) = -4\pi n_a s_d^3 W(s) [(s/s_d)^2 + 2(s/s_d) + 2].$$

Fig. 4 shows some typical examples of $SMR(s_1, s_2, \omega)$ calculations for different values of s_1 and s_2 . Note that, indeed, different wavelength bands give rise to different frequency behaviour of the SMR.

2.2. Calculation of the spectral noise density. To calculate the spectral noise density SND of the luminescent transitions, we must take into account the stochastic excitation and recombination source functions $G(s, t)$ and $R(s, t)$, respectively (eq. 6a). In the calculations presented here, stimulated emission and self-absorption are neglected. Following the usual method to obtain the spectral noise density in the recombination rate¹²⁾ denoted by $S_{\Delta r}(f)$, we find with the help of eq. (6c):

$$\begin{aligned} S_{\Delta r}(f) = & \int_0^{\infty} \int_0^{\infty} T(s) T(s') \\ & \times \frac{S_{G(s, t), G(s', t)}(f) + S_{R(s, t), R(s', t)}(f)}{[\alpha(s') + j\omega][\alpha(s) - j\omega]} ds ds' \\ & + 2 \int_0^{\infty} \int_0^{\infty} T(s) \operatorname{Re}[S_{\Delta N(s, t), R(s', t)}(f)] ds ds' \\ & + \int_0^{\infty} \int_0^{\infty} S_{R(s, t), R(s', t)}(f) ds ds', \end{aligned} \quad (14a)$$

where ‘‘Re’’ means the ‘‘real part of’’ and $S_{x, y}$ denotes the cross-spectral noise density of x and y . Here it was assumed that $G(s, t)$ and $R(s', t)$ are uncorrelated for all values of s and s' .

To calculate $S_{G(s, t), G(s', t)}(f)$ we extend the results of Fijnaut¹⁰⁾ for the discrete case to the continuous process in space described here. Introducing $\langle g(s, t) \rangle ds = \beta(s) \bar{\phi} ds$, where $\bar{\phi}$ is the average number of electrons incident on the phosphor per second and $\beta(s) ds$ is the average number of donor electrons, created per incident electron; for donors with nearest acceptor between s and $s + ds$, we have:

$$S_{G(s, t), G(s', t)}(f) ds ds' = 2\beta(s) ds [\beta(s') + \delta(s - s')] \bar{\phi} ds', \quad (14b)$$

where δ is Dirac's delta function. (See appendix of ref. 10.) Using our assumption concerning the uniform excitation rate $g(t)$, we may write:

$$\langle \beta(s) \rangle = \beta [N_d(s) - \langle N(s, t) \rangle], \quad (14c)$$

where β is independent of s , given by $\beta = \langle g(t) \rangle / \bar{\phi}$.

Since the deexcitation processes are spontaneous, we postulate:

$$S_{R(s,t),R(s',t)}(f) = 2 \overline{r(s,t)} \delta(s-s'). \quad (14d)$$

We now find with the procedures of Zijlstra and Alkemade¹²⁾ from eqs. (6c) and (14d):

$$\text{Re}[S_{\Delta N(s,t),R(s',t)}(f)] = - \frac{\alpha(s,t)}{\alpha^2(s) + \omega^2} S_{R(s,t)}(f) \delta(s-s'). \quad (14e)$$

With the help of eqs. (14a, b, c, d, e) we now find:

$$\begin{aligned} S_{\Delta r}(f) &= 2\beta^2 \bar{\phi} \int_0^\infty \int_0^\infty \frac{T^2(s) T^2(s') [\alpha(s) \alpha(s') + \omega^2] N_d(s) N_d(s')}{\alpha(s) \alpha(s') [\alpha^2(s) + \omega^2] [\alpha^2(s') + \omega^2]} ds ds' \\ &+ 4\beta \bar{\phi} \int_0^\infty \frac{T^2(s) N_d(s) [T(s) - \alpha(s)]}{\alpha(s) [\alpha^2(s) + \omega^2]} ds \\ &+ 2\beta \bar{\phi} \int_0^\infty \frac{T(s) N_d(s)}{\alpha(s)} ds. \end{aligned} \quad (15)$$

If the luminescence radiation is detected by means of a photomultiplier with gain G and mean secondary emission factor per stage δ , the relative excess noise REN in the anode current i_a of the photomultiplier is given by¹¹⁾:

$$\frac{S(f) - S_0}{S_0} = \mu \frac{\delta - 1}{\delta} \left(\frac{Ge\lambda S_{\Delta r}}{2e\bar{i}_a} - 1 \right), \quad (16a)$$

where μ is the detection efficiency for the radiation under study (here assumed to be wavelength independent) and $-e$ the electron charge.

Considering small values of $\langle g(t) \rangle$, *i.e.* $\langle g(t) \rangle \ll T(s)$, we have

$$\bar{r} \equiv \int_0^\infty \beta \bar{\phi} \frac{T(s)}{\alpha(s)} N_d(s) ds \approx \beta \bar{\phi} N_d,$$

since $N_d(s) = N_d P(s)$ and $\alpha(s) \approx T(s)$. In this approximation we now find from eqs. (16a) and (15):

$$\begin{aligned} \frac{S(f) - S_0}{S_0} &= \beta \frac{\delta - 1}{\delta} \mu N_d \left\{ \left[\int_0^\infty \frac{T^2(s) P(s)}{\alpha^2(s) + \omega^2} ds \right]^2 \right. \\ &\left. + \left[\omega \int_0^\infty \frac{T^2(s) P(s) ds}{\alpha(s) [\alpha^2(s) + \omega^2]} \right]^2 \right\}. \end{aligned} \quad (16b)$$

Observe that eqs. (16b) and (8) have the same frequency dependence! Obviously, the noise in the excitation rate $S_{G(s,t),G(s',t)}$ is the most important contribution to the REN. Since this holds also in the SMR, we may expect that the REN for spectral bands out of the emission spectrum will have also the same frequency dependence of the SMR, at least if $\langle g(t) \rangle \ll T(s)$.

The value of eq. (16b) for $\omega = 0$ turns out to be $\beta N_d \mu (\delta - 1) / \delta$, where βN_d is the average number of luminescent transitions per incident electron. From the excess-noise measurements and the values of μ and δ the number of photons per incident electron βN_d can be found without knowledge of the incident electron flux.

2.3. Calculation of the emission spectrum for continuous excitation. In the following calculations the influence of phonon interaction on the emission spectrum has been omitted. In addition, we assume here, as in the foregoing sections, that donors and acceptors are distributed randomly over the phosphor. Considering the recombination rate of donor electrons with acceptor holes at a distance between s and $s + ds$, denoted by $L(s) ds$, we must take into account contributions to $L(s) ds$ of donors with nearest acceptor at distance $s' < s$, each with transition probability to an acceptor between s and $s + ds$ of $4\pi n_a s^2 ds W(s)/T(s)$ [see eqs. (2) and (4)], and contributions of donors with nearest acceptor between s and $s + ds$, each with probability $W(s)/T(s)$. Then, we have:

$$L(s) ds = \int_0^s \frac{\overline{r(s', t)}}{T(s')} ds' 4\pi n_a s^2 ds W(s) + \overline{r(s, t)} \frac{W(s)}{T(s)} ds. \quad (17a)$$

Bearing in mind that $\overline{r(s, t)} = T(s) \overline{N(s, t)}$, eq. (5b), we find, with the help of eqs. (6b) and (7b) and $N_d(s) = N_d P(s)$:

$$L(s) ds = 4\pi n_a N_d s^2 W(s) ds \int_0^s \frac{\langle g(t) \rangle P(s')}{\alpha(s')} ds' + N_d \langle g(t) \rangle \frac{W(s) P(s)}{\alpha(s)} ds. \quad (17b)$$

In the limiting case of total saturation, *i.e.* $\langle g(t) \rangle \gg T(s)$, eq. (17b) reduces to $L(s) ds = 4\pi n_a N_d s^2 W(s) ds$, which result has also been found by Thomas *et al.*²⁾ The relation between wavelength λ and s can be found from eq. (1) by using $E = hc/\lambda$, where h is Planck's constant and c the velocity of light, and turns out to be:

$$\lambda = \frac{\lambda_m s}{(s + q) \lambda_m} \equiv A(s),$$

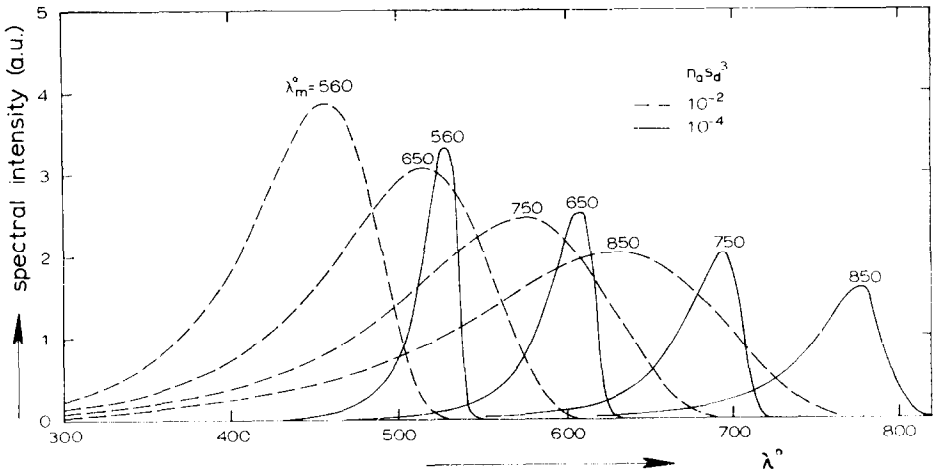


Fig. 5. Emission spectra calculated on the basis of eq. (18). For different values of $\lambda_m^0 = \lambda_m/s_d$ and $n_0 s_d^3$ the spectral emission intensity $L(\lambda)$ is plotted as function of $\lambda = \lambda/s_d$ in the limiting case $\langle g(t) \rangle \ll T(s)$.

where λ_m is the wavelength corresponding with $s \rightarrow \infty$; $q = e^2/(ehc)$. The recombination rate as a function of λ , $L(\lambda) d\lambda$ is now found to be:

$$L(\lambda) d\lambda = L(s) \frac{(s + \lambda_m q)^2}{\lambda_m^2 q} \Big|_{s=A^{-1}(\lambda)} ds. \quad (18)$$

Some numerically obtained results of emission spectra are shown in fig. 5, in the limiting case that $\langle g(t) \rangle \ll T(s)$, *i.e.*, for weak excitation as a function of the relative quantities $\lambda_m^0 = \lambda_m/s_d$ and $\lambda^0 = \lambda/s_d$.

3. *Experimental arrangement and results.* The experimental setup for measurement of modulation response and excess noise has been described by Fijnaut and Zijlstra¹¹). The experiments concerning selected wavelength bands were performed by means of interference filters of about 150 Å half-peak width. Spectral analysis of the emitted light was achieved by a monochromator with resolution of 5 Å. Experiments were carried out on two ZnS-Ag phosphors; one stemming from the Philips Natuurkundig Laboratorium, the other backed up on the screen of a R.C.A. 5WP 11 cathode ray tube. The concentration of Ag is about 10^{18} cm^{-3} , whereas neither the concentration nor the identity of the donor are known. However, since we are dealing with the green Cu-type luminescence, the donor concentration equals approximately the Ag concentration, while the donor should be a III b or VII b element.

The emission spectrum of the Philips-type phosphor, measured for a weak excitation density, *i.e.* $\langle g(t) \rangle$ small with respect to $T(s)$ is shown in fig. 6. Comparison of figs. 5 and 6 shows that in the first instance the agreement

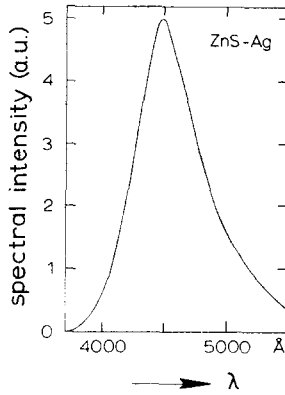


Fig. 6. Emission spectrum of ZnS-Ag, with spectral resolution of 5 \AA , for $\langle g(t) \rangle \ll T(s)$.

between theory and experiment is not imposing: the tail in the experimental curve extends towards the long-wavelength side of the maximum, whereas the theoretical curves show just the reverse behaviour. Here, however, the effect of phonon interaction should be borne in mind. Since our experiments were carried out at room temperature there is bound to be phonon interaction, giving rise to spectral broadening towards longer wavelengths³). In addition, Thomas *et al.*²) have remarked that eqs. (1) and (2) do not hold for small values of s , resulting in deviations between theory and experiments

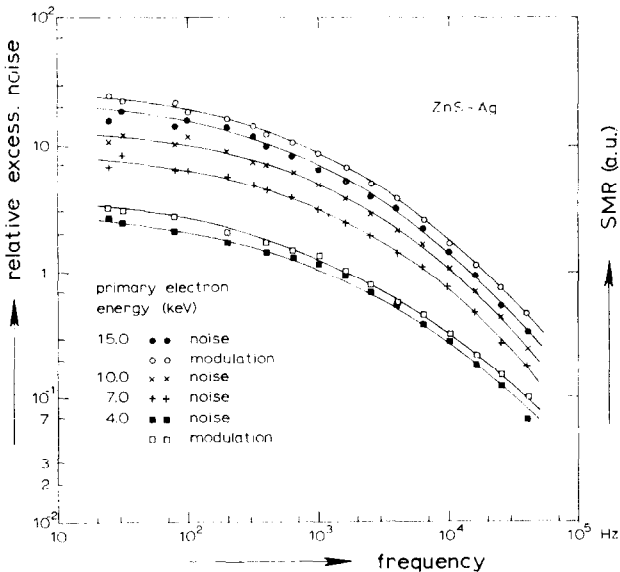


Fig. 7. Squared modulation response and relative excess-noise measurements of the integral emission of ZnS-Ag as a function of frequency, at different values of primary electron energy (Philips phosphor).

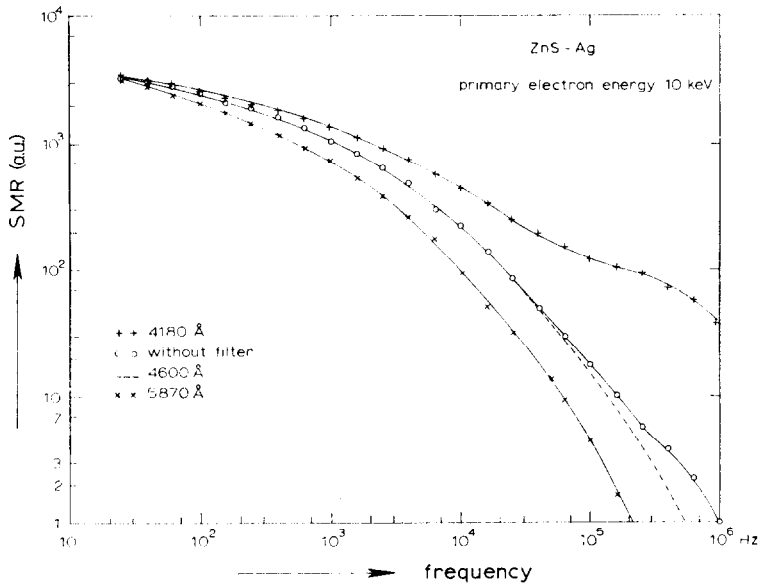


Fig. 8. SMR for different wavelength intervals as a function of modulation frequency. The interference filters used have a half-width of about 150 Å (Philips phosphor).

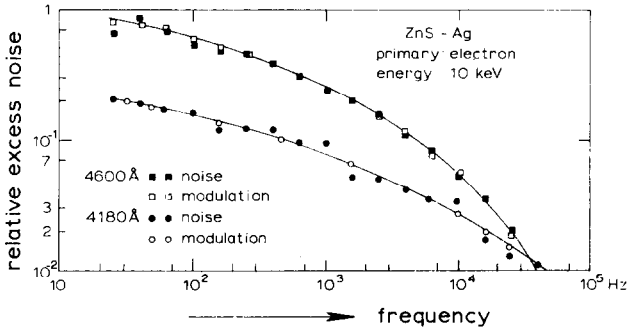


Fig. 9. SMR and relative excess noise for two wavelength bands as a function of frequency (Philips phosphor).

at shorter wavelengths. However, it seems of interest, according to Thomas, to compare shifts in peak position under increasing excitation densities. Therefore, in section 4 the peak shift calculated by us will be compared with the experimental results of Era *et al.*³⁾.

Some experimental results of the squared modulation response and excess noise measurements (Philips phosphor) are shown in fig. 7. The curves were obtained for the integral emission spectrum under weak excitation density. Note the mutual good agreement between SMR and excess noise, as far as frequency dependence is concerned, which is in accordance with theory.

The frequency dependence changes somewhat with primary-electron energy, indicating a variable acceptor concentration with depth in the phosphor. The increase in the relative excess noise, at fixed frequency, with increasing electron energy is associated with the increasing number of photons created per incident electron with energy. In addition, note the fairly slow decrease with frequency of the SMR and excess noise, as predicted by the theory, in contrast with, *e.g.*, the results for a CMT 7 phosphor¹¹⁾, which has an emission spectrum of about the same half-peak width, while the a.c. behaviour could be described with a single relaxation time. The RCA phosphor revealed quite a similar behaviour.

Fig. 8 shows the SMR measurements for selected spectral bands (Philips phosphor). It is clear that the frequency dependence varies with the central wavelength of the band.

In addition, noise measurements for two different spectral bands were performed and results are given in fig. 9. The mutual agreement between frequency dependence of excess noise and SMR is again in accordance with our theory.

4. *Discussion.* Owing to the lack of our own measurements of the emission spectrum under varying excitation densities, the theoretical results of section 2.3 may be compared with the experimental results of other authors. Era *et al.*³⁾ have found a shift in the wavelength of peak emission, corresponding to a shift in energy of 0.1 eV towards higher energies, when the excitation density was increased by a factor 10^6 . This has been found for a blue ZnS–Ag phosphor with acceptor concentration of 10^{18} cm^{-3} . Fig. 10 represents the theoretical peak shift with excitation density for $n_a = 10^{18} \text{ cm}^{-3}$, $s_d = 8.6 \text{ \AA}$ and peak energy 2.705 eV at low excitation density, *i.e.* λ^0 peak ≈ 520 , corresponding with $\lambda_m \approx 5150 \text{ \AA}$ (see fig. 5). The same figure shows the experimental results found by Era. The agreement between these relative changes is reasonable, although the measured shape of the spectrum differs

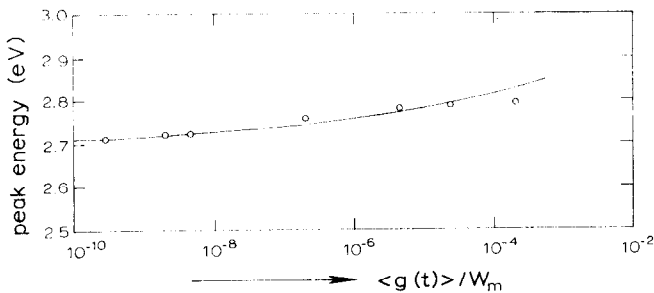


Fig. 10. Drawn curve: theoretical peak energy of the emission as a function of the excitation density, for $n_a = 10^{18} \text{ cm}^{-3}$ and $s_d = 8.6 \text{ \AA}$; \circ : experimental values of Era *et al.*³⁾ fitted by a shift along the horizontal axis.

from theoretical predictions. In the case of GaP, an analogous behaviour has been found by Thomas *et al.*²⁾.

The assumption of a random distribution of donors and acceptors, made in our calculations, seems reasonable, since the emission spectrum of fig. 6 does not show an extra short-wavelength bump, as predicted by Williams⁹⁾ for the case of associated donor-acceptor pairs.

In fig. 11 the SMR of the integral emission spectrum from the R.C.A. phosphor is compared with theory. Exact comparison with the SMR found from eq. (8) is not possible in view of the wavelength-dependent quantum efficiency of the photodetector. Nor can the numerical calculations of the SMR of eq. (12) be compared precisely with the experiments, since the function $f(s)$ chosen to approximate the quantum efficiency of the S 20 photocathode exaggerates the wavelength dependence of the quantum efficiency at wavelengths smaller than 4500 Å. In reality, the frequency dependence of the experimentally found SMR at a certain value of $n_a s_d^3$, will be a golden mean between the numerical calculations of the SMR's of eqs. (8) and (12) at corresponding values of $n_a s_d^3$. In fact, comparison with the experiments was done by shifting double log plots of calculated curves over the experimental ones until the best fit was obtained. Two theoretical curves are shown in fig. 11. From these curves we conclude that $10^{-4} < n_a s_d^3 < 10^{-3}$. Comparing the shapes of theoretical and experimental emission spectra, leaving out the long-wavelength tail (phonon interaction!), we find that λ_m^0 lies between 550 and 600. Then λ_{peak}^0 should lie between 500 and 560 for the range of $n_a s_d^3$ values considered. Since the experimental value of λ_{peak} is 4500 Å, we finally find $8 < s_d < 9$ Å, and thus $1.4 \times 10^{17} < n_a < 2 \times 10^{18}$ cm⁻³, which is reasonable since the Ag concentration is about 10^{+18} cm⁻³

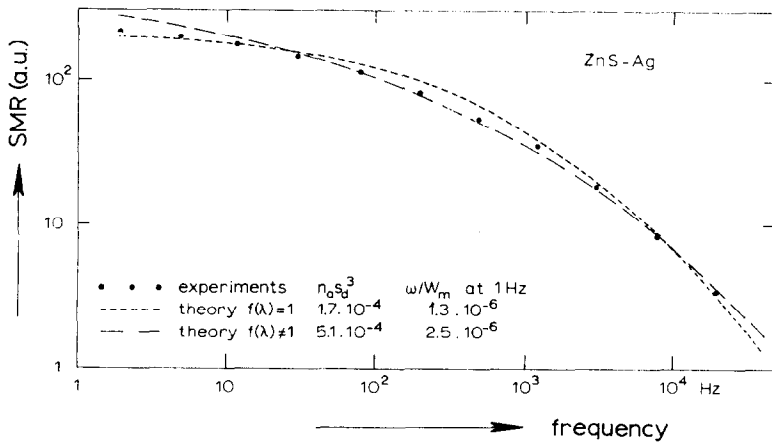


Fig. 11. Comparison of measured SMR as a function of frequency (...) with theoretical curves (R.C.A. phosphor). Here $f(\lambda) \equiv 1$ and $f(\lambda) \equiv a\lambda + b$.

(Bril, private communication). The value of W_m ²⁾ is found by fitting the horizontal axis of the theoretical SMR curves with the experimental curve. From the curves in fig. 11 it is found that $W_m \approx 10^6 \text{ s}^{-1}$. Thomas *et al.*²⁾ have found for GaP: $W_m = 10^6 \text{ s}^{-1}$ and $s_d = 12 \text{ \AA}$. Era *et al.*³⁾ assumed $W_m = 10^6 \text{ s}^{-1}$ and $s_d = 12 \text{ \AA}$, although they did not present arguments to support this choice. We may conclude that the SMR and noise measurements on the integral emission spectrum and the peak shift of the emission under varying excitation density of ZnS–Ag can be quantitatively or at least qualitatively, understood on the basis of donor-acceptor recombination.

The experimental results of the SMR for wavelength bands (fig. 8), however, show only qualitative agreement with theory (fig. 4). Different wavelength bands give differences in frequency behaviour, but the frequency dependence of the SMR on each such band is flattened out over a larger frequency range than predicted by theory (see figs. 4 and 8). Even when wavelength bands were selected by means of a monochromator, the same flattening was found. This effect can be explained by phonon interaction. In this case the relation between λ and s , derived in section 2.3, is not correct, since the energy associated with transitions between donors and acceptors at separation s is only partly transformed into radiation energy, giving rise to emission of longer wavelengths than predicted in section 2.3. Note that phonon interaction does not affect the SMR of the integral emission given by eq. (8), as can be seen immediately. Here, however, extra complications in the comparison of theory and experiment arise, when the quantum efficiency of the photodetector depends on λ .

The explanation of our results, based on donor-acceptor recombination should be weighed against an explanation based on the occurrence of traps from which transitions to the Ag acceptor could take place. Of course it might be possible to suggest the existence of such a particular set of traps with a specific transition probability distribution which could explain the measured SMR curves for the integral emission. However, it would be more difficult and arbitrary to choose a distribution, which could account for our SMR curves for selected wavelength bands. Moreover, the shift in emission peak with varying excitation density remains then still to be explained.

In conclusion, it may be stated that the results of our kinetic measurements corroborate the suggestion of Era *et al.*³⁾, that the luminescence of blue ZnS–Ag is caused by donor-acceptor recombination.

Acknowledgements. The authors are very much indebted to Drs. J. S. van Dieten for performing some of the measurements. The stimulating interest and the critical reading of the manuscript by Professor C. T. J.

Alkemade and Dr. R. J. J. Zijlstra are greatly appreciated. Our investigations were part of the work supported by the Foundation for Fundamental Research of Matter (F.O.M.).

REFERENCES

- 1) Williams, F. E., *J. Phys. Chem. Solids* **12** (1960) 265.
- 2) Thomas, D. G., Hopfield, J. J. and Augustyniak, W. M., *Phys. Rev.* **140** (1965) A202.
- 3) Era, K., Shionoya, S., Washizawa, Y. and Ohmatsu, H., *J. Phys. Chem. Solids* **29** (1968) 1827.
- 4) Van Gool, W., *Philips Res. Rep. Suppl.* **3** (1961) 1.
- 5) Shionoya, S., *Luminescence of lattices of ZnS type*, in: *Luminescence of Inorganic Solids*, ed. P. Goldberg, Academic Press (New York, 1966).
- 6) Shionoya, S., *J. of Luminescence* **1** (1970) 17.
- 7) Prener, S. J. and Williams, F. E., *J. Electrochem. Soc.* **103** (1956) 342.
- 8) Apple, E. F. and Williams, F. E., *J. Electrochem. Soc.* **106** (1959) 224.
- 9) Williams, F. E., *Phys. Status solidi* **25** (1968) 493.
- 10) Fijnaut, H. M., *J. Phys. D: Appl. Phys.* **4** (1971) 840.
- 11) Fijnaut, H. M. and Zijlstra, R. J. J., *J. Phys. D: Appl. Phys.* **3** (1970) 45.
- 12) Zijlstra, R. J. J. and Alkemade, C. Th. J., *Physica* **31** (1965) 1486.
- 13) Ubbink, J. T., thesis, Rijksuniversiteit Utrecht (1971).